

- 1968), chap. 5.1, pp. 121–125.
13. C. W. Bunn and E. R. Howells, *Nature* 174, 549 (1954).
 14. E. S. Clark and L. T. Muus, *Z. Kristallogr.* 117, 119 (1962).
 15. Value based on ab initio molecular orbital calculations on perfluoro-*n*-alkane chains by D. A. Dixon, F. A. van Catledge, B. E. Smart, Abstracts of the 9th International Union of Physical and Applied Chemistry Conference on Physical and Organic Chemistry (1988), p. A15.
 16. The extended zigzag conformation of PTFE in a more closely packed arrangement may be obtained in a B-centered cell with $a = 9.50 \text{ \AA}$, $b = 5.05 \text{ \AA}$, $\gamma = 105.5^\circ$, molecular area = 23.1 \AA^2 , but only at a pressure of at least 450 GPa; see H. D. Flack, *J. Polym. Sci. Part A-2* 10, 1799 (1972).
 17. Z. Berkovitch-Yellin, *J. Am. Chem. Soc.* 107, 8239 (1985).
 18. K. Kjaer *et al.*, in preparation.
 19. S. W. Barton *et al.*, *J. Chem. Phys.*, in press.
 20. We thank J. B. Lando for discussions and F. Hirsh-

feld for critical reading of the manuscript. Supported by the U.S./Israel Binational Science Foundation, Jerusalem; the fund for basic research of the Israel Academy of Sciences and Humanities; Stiftung Volkswagenwerk; the Petroleum Fund of the American Chemical Society; and the Danish Foundation for Natural Sciences. We gratefully acknowledge beam time at HasyLab, DESY, Hamburg, FRG.

1 June 1988; accepted 7 September 1988

Sugar and Signal-Transducer Binding Sites of the *Escherichia coli* Galactose Chemoreceptor Protein

NAND K. VYAS, MEENAKSHI N. VYAS, FLORANTE A. QUIOCHO

D-Galactose-binding (or chemoreceptor) protein of *Escherichia coli* serves as an initial component for both chemotaxis towards galactose and glucose and high-affinity active transport of the two sugars. Well-refined x-ray structures of the liganded forms of the wild-type and a mutant protein isolated from a strain defective in chemotaxis but fully competent in transport have provided a molecular view of the sugar-binding site and of a site for interacting with the Trg transmembrane signal transducer. The geometry of the sugar-binding site, located in the cleft between the two lobes of the bilobate protein, is novel in that it is designed for tight binding and sequestering of either the α or β anomer of the D-stereoisomer of the 4-epimers galactose and glucose. Binding specificity and affinity are conferred primarily by polar planar side-chain residues that form intricate networks of cooperative and bidentate hydrogen bonds with the sugar substrates, and secondarily by aromatic residues that sandwich the pyranose ring. Each of the pairs of anomeric hydroxyls and epimeric hydroxyls is recognized by a distinct Asp residue. The site for interaction with the transducer is about 18 Å from the sugar-binding site. Mutation of Gly⁷⁴ to Asp at this site, concomitant with considerable changes in the local ordered water structures, contributes to the lack of productive interaction with the transmembrane signal transducer.

BACTERIAL PERIPLASMIC BINDING proteins are essential components of both high-affinity active-transport systems and chemotaxis (1, 2). These proteins have three distinct binding sites that can be studied by x-ray crystallography: (i) a fast-reacting and tight-affinity binding site for substrates such as carbohydrates, oxyacid anions, or amino acids (3), (ii) a site (or a set of sites) for interacting with other transport protein components lodged in the cytoplasmic membrane, and (iii) a set of sites for interacting with the transmembrane signal transducer protein that is responsible for triggering chemotaxis.

We have determined and crystallographically refined to R-factor values of 0.15 to 0.18 the 1.7 Å structures of the L-arabi-

nose-binding (ABP) and sulfate-binding proteins and the 2.4 Å structures of the leucine-isoleucine-valine- and leucine-specif-

ic binding proteins (4–8). Recently we determined the D-maltose-binding protein structure at 2.8 Å (9) and, as we report, the refinement of the D-galactose-binding protein at 1.9 Å. The tertiary structures of the six proteins, representing about a third of the entire family of binding proteins, are similar despite minimal sequence homology; they are ellipsoidal and are composed of two distinct but similar globular domains that are connected by three separate peptide segments (for example, Fig. 1). The single substrate-binding site of each protein is located in an essentially identical cleft between the two domains. Perhaps the most striking common feature of these proteins is that the diverse substrates are bound mainly by hydrogen bonds (4, 5, 7, 9). These structural studies have also led to molecular understanding of protein-sugar interactions (10, 11) and of electrostatic interactions in protein structures and in binding of charged substrates (12).

To locate other functional sites, we stud-

Howard Hughes Medical Institute and Departments of Biochemistry and of Physiology and Molecular Biophysics, Baylor College of Medicine, Houston, TX 77030.

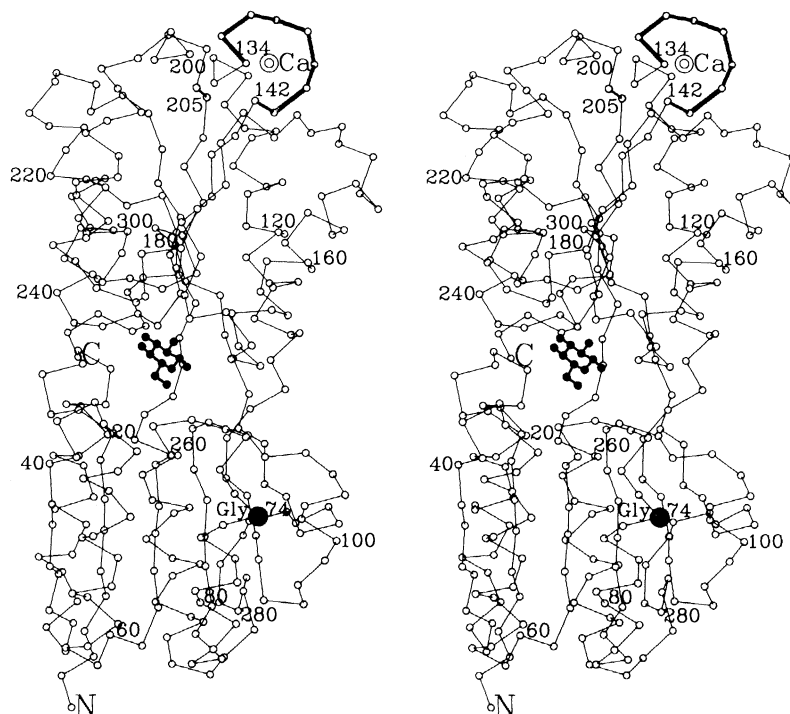
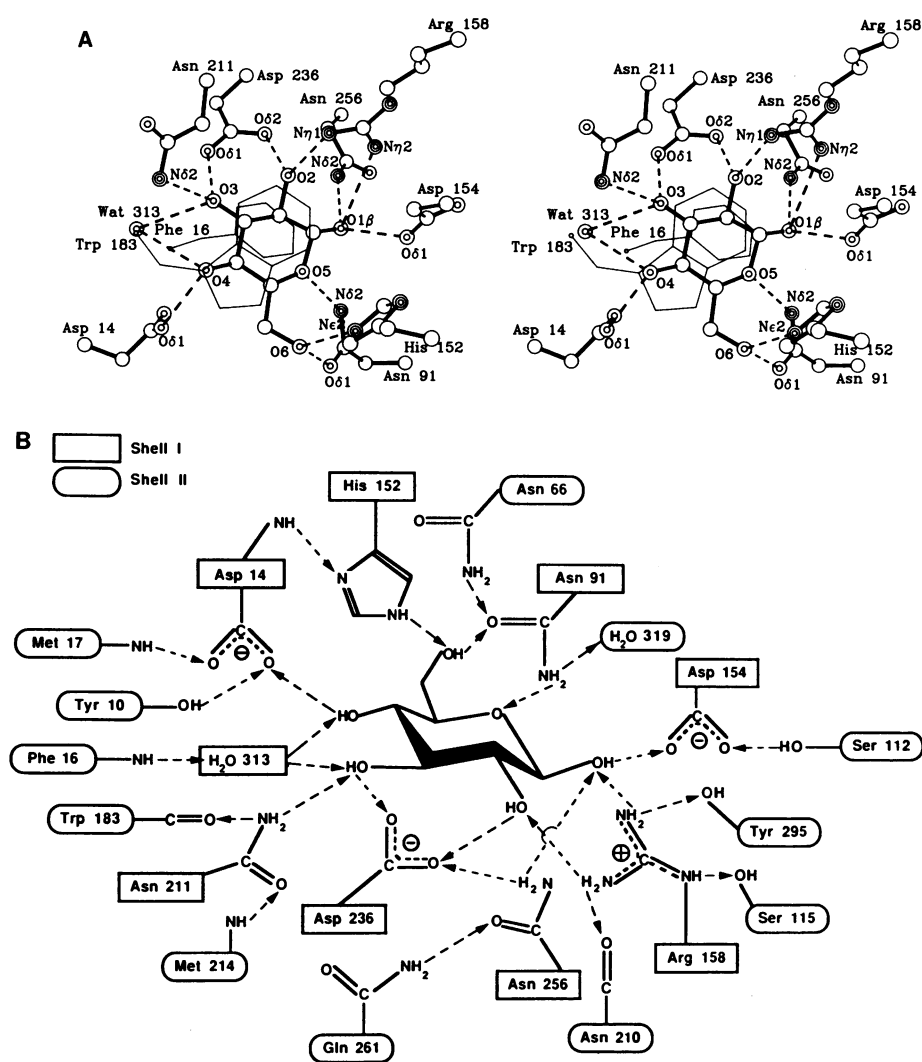


Fig. 1. α -Carbon backbone trace of the GBP structure refined at 1.9 Å resolution. Especially highlighted are: (i) the model of the β -D-glucose substrate (filled circles) buried in the cleft formed between the two domains; (ii) calcium (depicted as a double circle) bound in a loop (thicker lines) composed mainly of residues 134 to 142 located at one end of the elongated molecule [for details see (6)]; and (iii) Gly⁷⁴ (large filled circle), which is part of a site for interacting with the Trg transmembrane signal transducer. The orientation of the two domains is such that the amino termini of all the helices and carboxyl termini of all the strands point to the left between the two domains.

Fig. 2. (A) Stereoscopic view of the atomic interactions between GBP and D-glucose. Carbons are depicted as single circle, oxygens as double circles, and nitrogens as triple circles. The two binding-site aromatic residues (thin lines), Phe¹⁶ and Trp¹⁸³, sandwich the sugar. The OH4 is a hydrogen-bond donor to Asp¹⁴ Oδ1 and an acceptor from Water³¹³, which is the only exception to cooperative hydrogen bonding indicated in scheme 1, and may be important in sugar epimer binding (Fig. 4). Residues Arg¹⁵⁸ and Asp¹⁵⁴ are within salt-linking distance. Residues Asp¹⁴, Phe¹⁶, Asn⁹¹, and Asn²⁵⁶ are located in one domain and the residues His¹⁵², Asp¹⁵⁴, Trp¹⁸³, Arg¹⁵⁸, Asn²¹¹, and Asp²³⁶ are located in the other domain (Fig. 1). **(B)** Schematic diagram of the hydrogen bond network starting at the D-glucose and extending to two shells of residues. Residues in shell I are directly hydrogen bonded to the sugar and to other residues within the same shell. Residues in shell II hydrogen bond with those in shell I. The directions of the hydrogen bonds (arrows are from donors to acceptors) were dictated solely by the nature of the structure.



ied mutants of binding proteins that exhibit wild-type substrate binding in vitro, but that in vivo show a defect in either transport or chemotaxis, but not in both. Presumably the mutations affect the site or sites on the binding protein that interact with the membrane protein components for either transport or chemotaxis while leaving the substrate-binding site fully intact. One such mutant, a D-galactose-binding protein (GBP) isolated from strain AW551 of *Escherichia coli* K12 (GBP-551) (13), abolishes chemotaxis by disrupting the site for binding the Trg transmembrane signal transducer, but alters neither active transport (14, 15) nor sugar-binding activity of purified mutant protein (16).

Crystallographic refinements (17-21) of the structures of the liganded forms of the wild-type and AW551 mutant GBP not only solidified understanding of stereospecificity and affinity in protein-carbohydrate complexes, but also led to a partial elucidation of a site for interaction with the Trg signal transducer for galactose-glucose chemotaxis and a better comprehension of the effects of mutation on local conformation and ordered water molecules.

The refinement of the wild-type GBP crystal structure yielded an R-factor value of

Fig. 3. Stereo pair of the stacking of hydrophobic patches of the β-D-glucose (D-Glc) with the aromatic residues Phe¹⁶ and Trp¹⁸³. The individual van der Waals radii used for the molecular surfaces were C = 1.7 Å (green), N = 1.6 Å (blue), O = 1.5 Å (red). The sugar has hydrophobic surfaces or patches (green dots) and a polar surface (red dots). The major hydrophobic patch on the β or B face is composed of C3, C5, and C6 atoms, whereas the minor one on the α or A face is due to atoms C2 and C4.

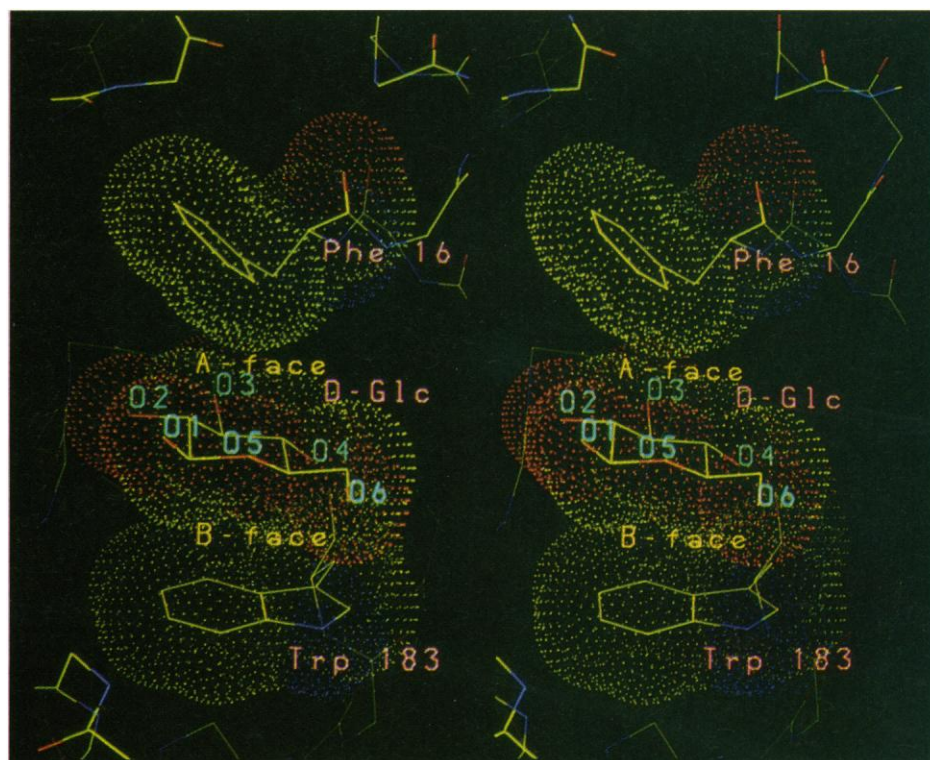


Fig. 4. Stereo view of the β -D-glucose (Glc, solid bonds) bound to GBP (Fig. 2A) superimposed on models of binding of α -D-glucose and α - or β -D-galactose (Gal) as derived by model-building experiments. The C–OH4 bond of the D-galactose and the C–OH1 bond of the α anomer are drawn in as hollow bonds. The hydrogen bonds determined from the x-ray structure are depicted as thick dashed lines and the hydrogen bonds from the modeling drawn as thin lines. Hydrogen bonds (not shown) involving OH2, OH3, O5, and OH6 of the sugar are identical to those shown in Fig. 2A. The total number and parameters of the hydrogen bonds and van der Waals contacts observed in the models of the binding of the epimer and the anomer are similar to those found in the refined GBP- β -D-glucose complex structure. These models were obtained without resorting to energy minimization or conformational idealization.

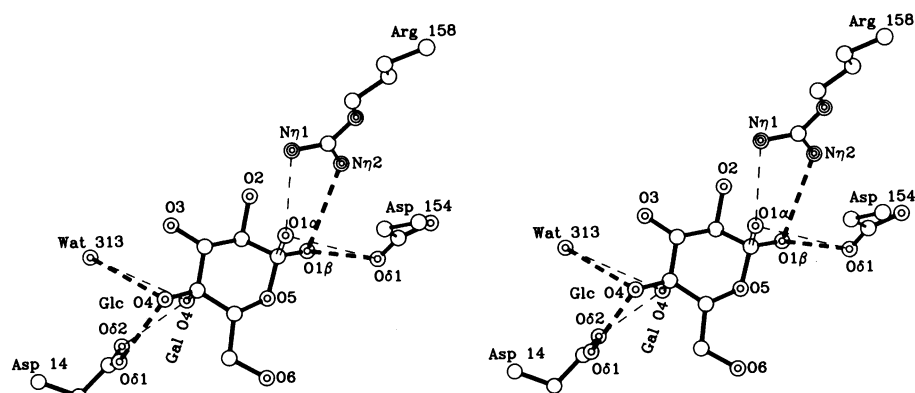
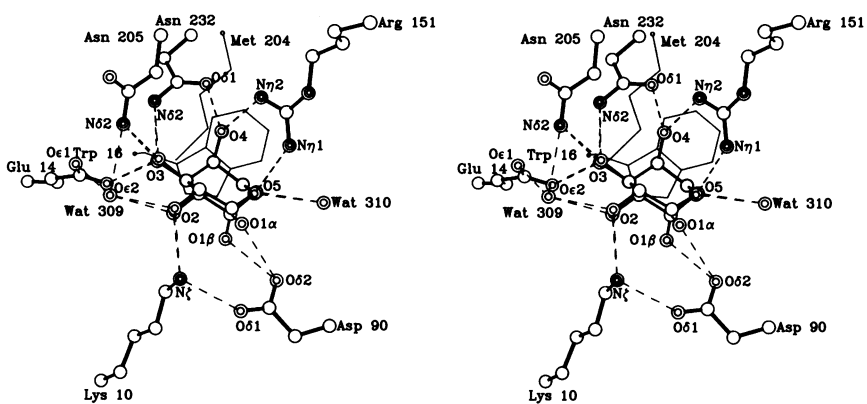


Fig. 5. Stereo view of the atomic interaction between L-arabinose-binding protein and L-arabinose as previously determined by refinement at 1.7 Å resolution (4). Besides the hydrogen bond interactions, there is partial stacking of the hydrophobic patch (C3, C4, and C5 atoms) located on the β face of the sugar with the β face of Trp¹⁶. The nonpolar C2 atom on the α face of the sugar is near the ϵ -CH₃ group of Met²⁰⁴. Structure refinement also shows that α or β anomer of the sugar is bound. Lys¹⁰ and Asp⁹⁰ are within salt-linking distance. Both Figs. 2A and 5 are oriented to present similar aspects to the viewer. Although many of the residues in both binding sites are identical or highly homologous, the different orientations of the sugars make the hydrogen-bonding interactions in both complexes different. Thus the prediction of Argos *et al.* (32) of the hydrogen bonding between GBP and D-galactose is incorrect.



0.146 by using all 19,531 observable reflections ($I/\sigma I > 0$) from 10 to 1.9 Å resolution. The final coordinates of all 2348 non-hydrogen atoms of the protein deviate from ideal bond lengths by 0.024 Å and ideal angle distances by 0.045 Å.

Since purified GBP contains bound endogenous D-glucose (22), which is also an excellent substrate (14, 15, 22, 23), refinement also revealed the atomic interactions between the protein and this monosaccharide (Figs. 1 to 3). The bound sugar is completely engulfed in the cleft between the two domains. The well-resolved electron density of the bound sugar shows preferential binding of β -D-glucose in the ⁴C₁ conformation (with χ_5 or C4–C5–C6–O6 torsion angle of 177°). No other density near the C1 sugar atom clearly indicates the binding of the α anomer, but the presence of a small fraction (<30%) of this form is not easily demonstrable by the present refinement technique (24).

The buried D-glucose forms 13 strong hydrogen bonds involving eight polar side chains distributed between the two domains and a water molecule (Fig. 2). All of the hydroxyls and the ring oxygen of the D-glucose participate in hydrogen bonding. The hydroxyls do so “cooperatively” by

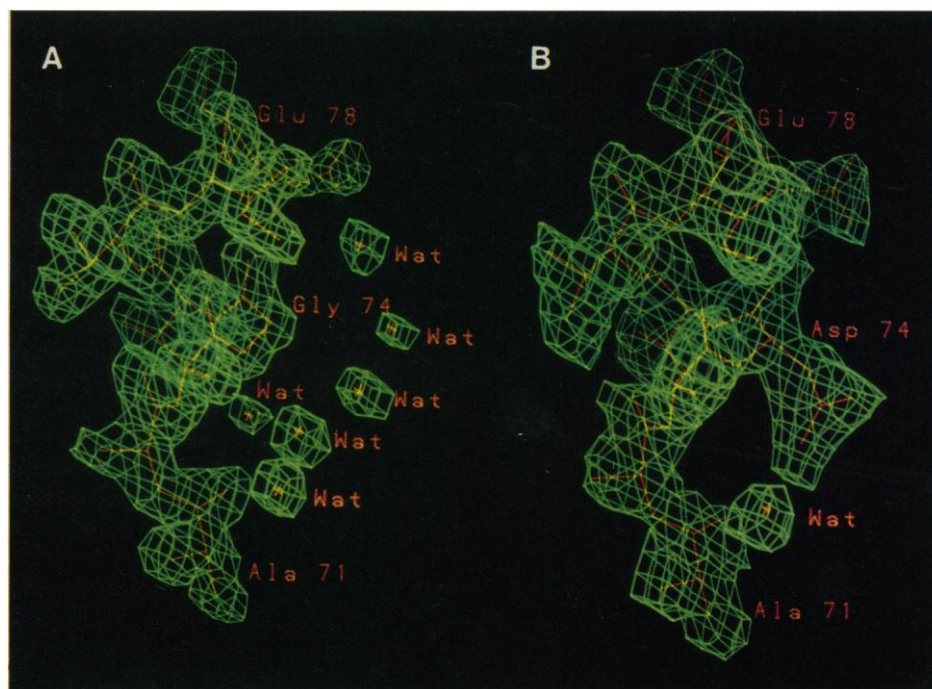


Fig. 6. Refined structures (orange) of the (A) wild-type GBP (Gly⁷⁴) and (B) GBP-551 (Asp⁷⁴) in the immediate vicinity of residue 74 superimposed on the electron density map (green). The wild-type structure contoured at 0.35 electron Å⁻³. Also shown are six bound water (Wat) molecules near Gly⁷⁴. The GBP-551 structure contoured at 0.25 electron Å⁻³. Asp⁷⁴ and nearby residues are clearly resolved even at 3 Å resolution, and all but one of the water molecules present in the wild type are absent.

simultaneously donating and accepting hydrogen bonds. These cooperative hydrogen bonds can be depicted as:



where the NH group is the hydrogen bond donor and the O atom is the acceptor group of side chains, OH is a sugar hydroxyl, and $n = 1$ or 2. The mean of 2.87 (0.28) Å of the distances between the donors and acceptors indicates strong hydrogen bonds overall in the GBP-glucose complex. The mean of the hydrogen bond angles is 156 (16)°, but the strength of hydrogen bonds varies mainly with distance and only slightly with small bending of the angle from the mean.

All of the side chains of the eight residues used in hydrogen bonding the sugar have planar structure and at least two polar groups (Fig. 2). Five factors account for this finding: (i) These residues contain the NH and O groups used for cooperative hydrogen bonding. (ii) All eight residues are fixed by intramolecular hydrogen bonding and, moreover, their hydrogen-bonding groups do not have freedom of torsional rotation. The final geometry of the binding site depends on the final folded protein and any ligand-induced conformational change that brings these residues to their correct positions. (iii) Three residues (Asn⁹¹, Arg¹⁵⁸, and Asp²³⁶) form favorable bidentate hydrogen bonds with the glucose (Fig. 2A). The O2 and O3 atoms of the sugar and Oδ1 and Oδ2 of Asp²³⁶ are coplanar, as are the group of atoms O6 and O5 of the sugar and Oδ1 and Nδ2 of Asn⁹¹. There is less coplanarity of atoms O1 and O2 of the sugar and Nη1 and Nη2 of Arg¹⁵⁸. (iv) All of the planar polar side chains form extensive networks of hydrogen bonds with other residues in the binding site region (Fig. 2B). All of the hydrogen-bonding groups (either as donors or acceptors) of the side chains and the glucose molecule are used in the formation of cooperative, bidentate, and networked hydrogen bonds. (v) Carboxylate side chains are important in binding sugar anomers and specific epimers (see below).

Many of the cooperative hydrogen bonds exhibit nearly ideal geometries. The coordinations of OH1 and OH3 are essentially tetrahedral, including the sugar C–O bond. The hydrogen-bonding geometry of OH2, simultaneously donating and accepting one hydrogen bond, is such that the atoms C2 and O2 of the sugar, Arg¹⁵⁸ Nη1 and Asp²³⁶ Oδ2, are coplanar. Furthermore, since the Arg¹⁵⁸ Nη1H group donated to the OH2 is in a direction that bisects both sp^3 lone pairs of electrons (in their predicted orientations) on the hydroxyl oxygen, both lone pairs likely share in accepting the hydrogen bond, as is the case with OH6 and O5.

There are ~60 van der Waals contacts (3.3 to 4.0 Å) between all of the non-hydrogen atoms of the sugar and 12 residues and four ordered water molecules. Of these, 42 contacts result from hydrogen-bonding interactions, enabling more of the atoms of the polar residues to come within van der Waals distance of the sugar. Stacking of both sides of the glucopyranose ring with aromatic residues (Figs. 2A and 3) produces only nine contacts. [To distinguish the two faces or sides of the pyranose ring of the ⁴C₁ conformation and the indole ring of tryptophans, we use the α/β or A/B convention for cyclic compounds (25).] In the GBP-glucose complex, the α face of the sugar is partially stacked with Phe¹⁶ from the N-domain, whereas the β face is completely covered by the α face of Trp¹⁸³ from the C-domain (Fig. 3).

The geometry and nature of the binding are fully consistent with the unusual substrate specificity and other ligand-binding properties of GBP. For example, the 4-epimers D-galactose and D-glucose are both excellent substrates of GBP, and the α and β anomers of these sugars can bind with indistinguishable properties (3, 22). Based on model-building experiments with PSFRODO, the site can bind D-galactose and D-glucose in almost exactly the same mode, except that the axial OH4 of the galactose is donated to Oδ2 of Asp¹⁴ (hydrogen bond distance = 2.8 Å, angle = 168°), instead of to Oδ1 of the same residue (Fig. 4). Asp¹⁵⁴ is equally crucial because, like Asp⁹⁰ in ABP [see Fig. 5 and (4)], its Oδ1 atom can form a hydrogen bond with either the α- or β-anomeric hydroxyl of both D-galactose and D-glucose (Fig. 4). Precise positioning of Asp¹⁵⁴ of GBP and Asp⁹⁰ of ABP is achieved through charge-coupling and hydrogen-bonding interactions with basic residues (Figs. 2A and 5). These stereospecificities show that GBP has an antipodal sugar-binding site; at one end is the epimeric recognition subsite, and at the opposite end is the anomeric recognition subsite, each subsite requiring a separate Asp residue (Fig. 4). The types of residues interacting with the monopyranosides (Figs. 2A, 3, and 4) are also consistent with the observations that sugar binding induces a change in the Trp fluorescence (22, 26), and is unaffected by pH, from pH 5.5 to 9.5 (23).

When two adjacent hydroxyls of pyranosides each interact with a different atom of the same planar polar side-chain residue, they formed bidentate hydrogen bonds, which require a pair of hydroxyls that are both equatorial (for example, the OH1 and OH2 pair and OH2 and OH3 pair of D-glucose; Fig. 2A) or one equatorial and the other axial (for example, OH3 and OH4 of

L-arabinose; Fig. 5). The sugar ring oxygen, when paired with OH6 of D-glucose in the χ^5 conformation shown (Fig. 2A) and OH4 of L-arabinose (Fig. 5) can also participate in bidentate hydrogen bonding (Figs. 2A and 5). In all five different cases cited, the distance between the pair of sugar oxygen atoms is about 2.8 Å, ideal for bidentate hydrogen bonds with the planar side chains.

Since planar, polar side-chain residues with at least two functional groups are the only ones participating in cooperative, bidentate, and networked hydrogen bonds, many of these residues are in the sugar-binding sites of ABP, GBP, and other proteins as well (10, 11). For recognition of the epimeric hydroxyls of D-galactose and D-glucose, each requires a different oxygen atom of the same carboxylate side chain of GBP (Fig. 4), whereas only one carboxylate oxygen atom is used for interacting both anomeric hydroxyls of the sugar substrates of ABP and GBP (Figs. 4 and 5). The protein-sugar interactions of GBP and ABP demonstrate stacking of aromatic side chains with the pyranose ring (Figs. 2A, 3, and 5). The D-glucopyranoside bound to GBP is sandwiched by phenyl and indolyl side chains, whereas only the β face of the L-arabinopyranoside bound to ABP is partially stacked with the β face of a Trp residue (Fig. 5). The pairings of all of the polar groups facilitate the stacking interaction, but also limit the nonpolar contacts. Of the 350 Å² total accessible surface area of β-D-glucose (27), only 20% represents nonpolar surface [C3, C5, and C6 on the β face and C2 and C4 on the α face (Figs. 1 and 3)]. L-Arabinose has only one major hydrophobic patch (C3, C4, and C5), which is located on the β face [see Fig. 5 and (4)], but note that the accessible nonpolar C2 atom on the α face is near an ε-CH₃ group of Met²⁰⁴ (Fig. 5) (16). The aromatic residues further contribute to the specificity by disallowing binding of other sugar epimers because of steric hindrance or unfavorable nonpolar environment or both. Indeed, only the D-galactose and D-glucose epimers are known to be the best substrates of GBP. L-Arabinose is the best substrate of ABP; the other epimers—L-ribose, L-xylose, and D-xylose—bind significantly less tightly (28).

Because of a ligand-induced conformational change, the essential residues poised in both domains are brought into interacting positions, and the bound sugar and all of the residues are buried and completely sequestered in the cleft between the two domains. The conformational change is described as a hinge-bending motion between the two domains or a "Pac-man" model (7, 29), with closure of the cleft preceded by the substrate binding first to one domain (7). As

expected of tight ligand binding in enclosed, solvent-inaccessible binding sites, all functional groups of polar residues and of every one of the potential hydrogen bond donor groups of these residues and the sugar are used, leading to the formation of extensive networks of hydrogen bonds and to precisely and stably positioned functional groups. The numerous, well-optimized hydrogen-bonding and van der Waals interactions in both binding protein-sugar complexes give rise to high packing efficiency of all atoms involved. Since the protein hydrogen-bonding groups have fewer degrees of freedom than water, they offer a more stable solvation shell for the bound substrates. Moreover, the lower dielectric constant within the solvent-excluding cleft sequestering the sugar is likely to strengthen hydrogen bonds.

Saccharides have a large (about 70%) polar surface composed of hydroxyl and ring oxygen groups and a smaller nonpolar surface roughly represented by the hydrophobic patches (see Figs. 2, 3, and 5). Favorable entropy contributions to the stability of protein-carbohydrate complexes are derived from both hydrophilic effects (expulsion of hydrogen-bonded water molecules) and hydrophobic effects (disordering of organized water structure). However, the x-ray structures and thermodynamic data indicate that hydrogen bonds and van der Waals contacts are major factors in the absolute stability of these complexes (10, 11).

The sequence of *mglB551*, which encodes GBP-551 (30), shows that Gly⁷⁴ of the wild type is replaced by Asp. As single crystals of the GBP-551 are isomorphous with the wild-type protein crystals (17), the side chain of Asp⁷⁴ was easily fitted to an initial electron density map of the mutant structure calculated with coefficients ($2|F_o| - |F_c|$, α_c), where initial phases α_c were due to the refined wild-type GBP structure. The complete mutant structure was then refined (17) to finally yield an *R*-factor of 0.155 for 5365 reflections ($I/\sigma I > 0$) in the resolution range 10 to 3 Å. The final coordinates deviate from ideal bond lengths by 0.020 Å and ideal angle distances by 0.059 Å. The region of electron density around residue 74 in the wild-type and the GBP-551 protein structures, respectively, is shown in Fig. 6. No gross protein structural changes accompany the mutation. Indeed, superimposing both structures yields root-mean-square deviations of 0.55 Å for all 2348 protein atoms, 0.30 Å for main-chain atoms only, and 0.1 Å for 309 α -carbon atoms only.

In the wild-type GBP structure, a string of water molecules commences in the middle of a shallow groove between the third α helix (residues 72 to 82) and the fourth helix (residues 95 to 100) in the N-domain and

eventually connects with a cluster of water molecules at the opening of the sugar-binding cleft. These water molecules are held in place by hydrogen bonds either to the protein or to each other. Six water molecules near residue 74 are shown in Fig. 6A. Gly⁷⁴ abuts the water-filled groove; only one of these water molecules remains after substitution by Asp and occupation of the groove by the Asp side chain (Fig. 6B), and a slight rotation of the side chain of Glu⁷⁸ about χ_1 and χ_2 occurs, which perturbs the salt link between Glu⁷⁸ and Arg⁸¹. This substitution probably accounts for the lack of productive interaction between GBP-551 and Trg. The expulsion of a large number of water molecules and small changes in the local structure might further affect the interaction.

Gly⁷⁴ is the third residue in the first turn of the third helix, which puts it near one of the "lips" of the sugar-binding cleft, but distant (~18 Å) from the nearest hydroxyl (OH6) of the bound glucose (Fig. 1). Thus purified GBP-551 exhibits wild-type sugar-binding activity (16), and strain AW551, although defective in chemotaxis, shows normal sugar-transport activity (14, 15). Moreover, the mutant and parent structures have sugar bound in exactly the same location. The immediate vicinity of Gly⁷⁴ does not participate in the interaction with MglA and MglC (2, 14, 15, 30).

We can obtain some clues as to the means by which the binding protein interacts with the portion of the membrane-bound Trg transducer extending into the periplasm. The area around Gly⁷⁴ is highly polar; within a 12 Å radius from Gly⁷⁴, there are 14 exposed residues, of which 11 are polar and 3 are nonpolar (Fig. 1). Only three residues (Asp⁶⁹, Ala⁷¹, and Gly⁷⁴) form 11 contacts of no greater than 4 Å with a neighboring molecule in the crystal lattice. There are salt link (between Asp⁶⁹ and Lys²⁹ of an adjacent molecule) and ten van der Waals contacts; no hydrogen bonds are observed. The groove located between the third and fourth helices, which contain the array of water molecules, could serve as a specific intercalation site for polar residues (such as Asp) on the corresponding site of the signal transducer. Furthermore, a favorable positive entropic effect resulting from the displacement of the ordered water molecules in the groove could provide the driving force in the formation of the GBP-Trg complex. No other comparable chain of water molecules could be found in GBP, although there are five other pairs of parallel helices (Fig. 1).

The similarity of the binding protein structures (especially the presence of the two lobes for interacting productively with membrane components and the deep cleft between the lobes for ligand binding), the

nature of the binding sites, and the ligand-binding properties of these proteins are essential for function in both active transport and chemotaxis (3-5, 7). Our studies further reinforce those of others (31), indicating the importance of high-resolution x-ray analysis for understanding the properties of mutant proteins. Finally, only by determining the ABP and GBP structures were we able to discover that, in spite of the high degree of structural and sequence homology of both sugar-binding sites, the exact hydrogen-bonding interactions in both complexes are not equivalent (Figs. 2 and 5).

REFERENCES AND NOTES

1. J. A. Adler, *Annu. Rev. Biochem.* **44**, 341 (1975); R. W. Macnab, in *Escherichia coli and Salmonella typhimurium: Cellular and Molecular Biology*, F. C. Neidhardt, Ed. (American Society for Microbiology, Washington, DC, 1987), pp. 732-759.
2. C. E. Furlong, in *Escherichia coli and Salmonella typhimurium: Cellular and Molecular Biology*, F. C. Neidhardt, Ed. (American Society for Microbiology, Washington, DC, 1987), pp. 768-796.
3. D. M. Miller III, J. S. Olson, J. W. Pflugrath, F. A. Quioco, *J. Biol. Chem.* **258**, 13665 (1983).
4. F. A. Quioco and N. K. Vyas, *Nature* **310**, 381 (1984).
5. J. W. Pflugrath and F. A. Quioco, *ibid.* **314**, 257 (1985); *J. Mol. Biol.* **200**, 163 (1988).
6. N. K. Vyas, M. N. Vyas, F. A. Quioco, *Nature* **327**, 635 (1987).
7. J. S. Sack, M. A. Saper, F. A. Quioco, *J. Mol. Biol.*, in press.
8. J. S. Sack, S. D. Trakhanov, I. Tsigannik, F. A. Quioco, *ibid.*, in press.
9. J. C. Spurlino, thesis, William Marsh Rice University, Houston, TX (1988); J. C. Spurlino, G.-Y. Lu, F. A. Quioco, unpublished data.
10. F. A. Quioco, *Annu. Rev. Biochem.* **55**, 287 (1986).
11. ———, *Curr. Top. Microbiol. Immunol.* **139**, 135 (1988); *Pure Appl. Chem.*, in press.
12. F. A. Quioco, J. S. Sack, N. K. Vyas, *Nature* **329**, 561 (1987).
13. GBP-551 was purified from *E. coli* K12 strain AW551 (14). The cells were grown to late log phase (15) and the mutant protein isolated with a procedure similar to ones used in the isolation of several binding proteins in our laboratory [for example, see (3)].
14. G. L. Hazelbauer and J. A. Adler, *Nature* **230**, 101 (1971).
15. G. W. Ordal and J. A. Adler, *J. Bacteriol.* **117**, 509 (1974).
16. F. A. Quioco, unpublished data.
17. Mutant GBP crystals were obtained by the same procedure as for the wild-type crystals (18). Both wild-type and mutant crystals belong to space group $P2_1$ and exhibit similar unit cell dimensions: wild-type, $a = 66.00$ Å, $b = 37.05$ Å, $c = 61.57$ Å, and $\beta = 106.8^\circ$; GBP-AW551, $a = 65.89$ Å, $b = 37.04$ Å, $c = 61.32$ Å, and $\beta = 107.5^\circ$. Measurement and processing of x-ray diffraction intensities from binding protein crystals are described in (5). The wild-type and mutant GBP structures were refined by alternating use of the PROLSQ restrained least-squares refinement program (19) (PROFFT version provided by B. C. Fenzel) and PSFRODO (20), an extensively modified version of FRODO (21) converted for the E&S PS300 computer graphics system and further enhanced by J. S. Sack in our laboratory.
18. F. A. Quioco and J. W. Pflugrath, *J. Biol. Chem.* **255**, 6559 (1980); N. K. Vyas, M. N. Vyas, F. A. Quioco, *Proc. Natl. Acad. Sci. U.S.A.* **80**, 1792 (1983).
19. W. A. Hendrickson and J. H. Kennert, in *Computing in Crystallography*, R. Diamond, S. Ramaseshan, K.

Venkateshan, Eds. (Indian Academy of Sciences, Bangalore, 1980), pp. 13.01–13.23.

20. J. W. Pflugrath, M. A. Saper, F. A. Quijoco, in *Methods and Application in Crystallographic Computing*, S. Hall and T. Ashida, Eds. (Clarendon, Oxford, 1984), pp. 404–407.

21. T. A. Jones, *J. Appl. Crystallogr.* **11**, 268 (1978).

22. D. M. Miller III, J. S. Olson, F. A. Quijoco, *J. Biol. Chem.* **255**, 2465 (1980).

23. Y. Anraku, *ibid.* **243**, 3116 (1968).

24. R. B. Honzatko, W. A. Hendrickson, W. E. Love, *J. Mol. Biol.* **184**, 147 (1985); J. L. Smith, W. A. Hendrickson, R. B. Honzatko, S. Sheriff, *Biochemistry* **25**, 5018 (1986).

25. I. A. Rose, K. R. Hanson, K. D. Wilkinson, M. J.

Wimmer, *Proc. Natl. Acad. Sci. U.S.A.* **77**, 2439 (1980).

26. R. G. Parson and R. W. Hogg, *J. Biol. Chem.* **249**, 3608 (1974).

27. B. Lee and F. M. Richards, *J. Mol. Biol.* **55**, 379 (1971). The program ACCESS used to calculate solvent-accessibility was provided by F. M. Richards.

28. R. W. Hogg and E. Englesberg, *J. Bacteriol.* **100**, 423 (1969); M. E. Newcomer, D. M. Miller III, F. A. Quijoco, *J. Biol. Chem.* **254**, 7529 (1979).

29. M. E. Newcomer, B. A. Lewis, F. A. Quijoco, *J. Biol. Chem.* **254**, 13218 (1981); B. Mao, M. R. Pear, J. A. McCammon, F. A. Quijoco, *ibid.* **257**, 1131 (1982).

30. A. Sholle *et al.*, *Mol. Gen. Genet.* **208**, 247 (1987).

31. T. Alber *et al.*, *Nature* **330**, 41 (1987); M. F. Perutz, G. Fermi, J. Fogg, S. Rahbar, *J. Mol. Biol.* **201**, 459 (1988).

32. P. Argos, W. C. Mahoney, M. A. Hermodson, M. Hanci, *J. Biol. Chem.* **256**, 4357 (1981).

33. We thank J. A. Adler for providing the *E. coli* strain AW551 and G.-Y. Lu for purifying and crystallizing the mutant protein. Supported by the Howard Hughes Medical Institute and grants from the National Institutes of Health and the Welch Foundation. Coordinates have been offered for deposit with the Brookhaven Data Bank.

18 May 1988; accepted 8 September 1988

Two Cytosolic Neutrophil Oxidase Components Absent in Autosomal Chronic Granulomatous Disease

BRYAN D. VOLPP, WILLIAM M. NAUSEEF, ROBERT A. CLARK*

Neutrophils kill microorganisms with oxygen radicals generated by an oxidase that uses the reduced form of nicotinamide adenine dinucleotide phosphate (NADPH) as substrate. This system requires both membrane and cytosolic components and is defective in patients with chronic granulomatous disease. A cytosolic complex capable of activating latent membrane oxidase was eluted from guanosine triphosphate-agarose and was used to raise polyclonal antiserum that recognized 47- and 67-kilodalton proteins. These proteins were restricted to the cytosol of myeloid cells. Both proteins were associated with NADPH oxidase-activating capacity when neutrophil cytosol was purified on nucleotide affinity matrices or molecular sizing columns. Neutrophils from patients with two different forms of autosomal chronic granulomatous disease lacked either the 47- or 67-kilodalton protein.

THE MICROBICIDAL ACTIVITY OF POLYMORPHONUCLEAR neutrophils (PMNs) depends on a burst of nonmitochondrial oxidative metabolism that converts molecular oxygen to superoxide anion and other toxic oxygen derivatives. The biochemical basis for this respiratory burst is the stimulus-dependent activation of an NADPH oxidase (1). This enzyme system consists of (i) membrane-associated catalytic components that include cytochrome b_{558} and function as an electron transport chain (2–4) as well as (ii) soluble cytosolic components that appear to be involved in oxidase activation (4, 5). Chronic granulomatous disease (CGD), a clinical syndrome of severe and recurrent infections, is characterized biochemically by the absence of the respiratory burst (1, 6). The X-linked form is associated in most cases with an absence of cytochrome b and an inherited defect in its 91-kD β subunit (1, 6, 7). In contrast, autosomal CGD, constituting about one-third of the cases, is generally characterized by normal cytochrome b but an absence of the essential cytosolic factor activity (8–10).

Several laboratories have used a system of subcellular components to reconstitute a functioning oxidase system *in vitro* (4, 5). In this cell-free system, the latent oxidase is activated and NADPH-dependent superox-

ide formation expressed when PMN plasma membrane or specific granule membrane fractions are combined with cytosol, Mg^{2+} , and either arachidonic acid or SDS. Activation of the reconstituted system is augmented by guanosine triphosphate (GTP) analogs or fluoride and inhibited by guanosine diphosphate (GDP) analogs, suggesting involvement of a GTP-binding protein (11). In addition, we have recently noted the presence of a substrate for pertussis toxin-catalyzed adenosine diphosphate (ADP)-ribosylation in PMN cytosol (12). On the basis of these observations, we reasoned that the cytosolic factor important in activation might be a GTP-binding protein and we attempted to purify this factor by GTP-agarose affinity chromatography. Fractions were assessed for superoxide-generating activity in the presence of PMN membrane fractions, arachidonic acid, and NADPH (Fig. 1). All of the activity in cytosol was bound to the column and was eluted with a

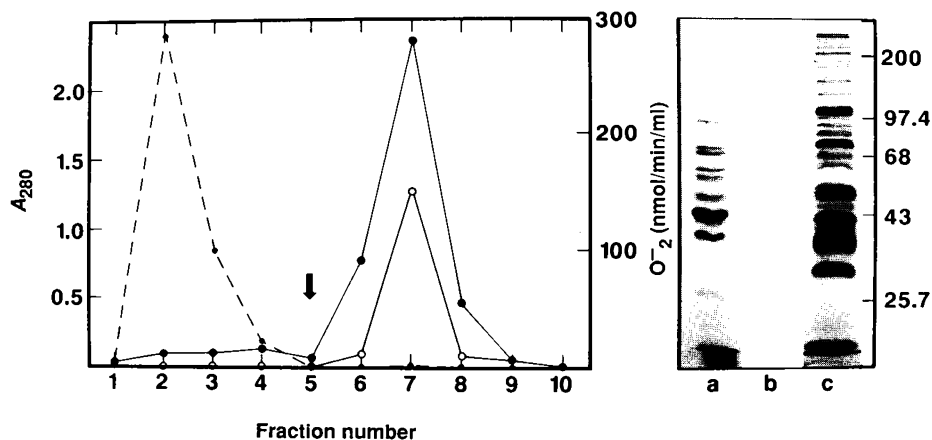


Fig. 1. Partial purification of PMN cytosol factor on a GTP-agarose affinity column. Human PMNs (18) were purified, disrupted by nitrogen cavitation, and fractionated on Percoll gradients (4). (Left) Cytosol from 2×10^8 cells was loaded on a column containing 1 ml of GTP-agarose (19). The column was then washed with 5 ml of buffer followed by elution with 5 ml of buffer (arrow) (19). Fractions of 1 ml were collected and assessed for protein (---) and NADPH oxidase activation (4, 20) (—) in the presence (●) or absence (○) of 5 μ M GTP- γ -S (Boehringer Mannheim). (Right) SDS-PAGE on 9% slab gels (21). Shown are Coomassie blue stains of (a) PMN cytosol (5×10^6 cell equivalents) and (b) the active fraction from the GTP-agarose column ($\sim 40 \times 10^6$ cell equivalents) and (c) a silver stain of the same quantity of the active column fraction. The locations of molecular size standards are shown in kilodaltons.

Department of Medicine, University of Iowa, College of Medicine, and Veterans Administration Medical Center, Iowa City, IA 52242.

*To whom correspondence should be addressed.